Arabian Journal of Chemistry (2021) **14**, 103090

King Saud University

Arabian Journal of Chemistry

www.ksu.edu.sa
www.sciencedirect.com

ORIGINAL ARTICLE

Room temperature and surfactant free synthesis of zinc peroxide (ZnO_2) nanoparticles in methanol with highly efficient antimicrobials

Hawkar M. Hussein [a], **Dlzar D. Ghafoor** [a,b,*], **Khalid M. Omer** [a,*]

[a] *Department of Chemistry, College of Science, University of Sulaimani, Qliasan st, 46002 Sulaimaniyah, Kurdistan Region, Iraq*
[b] *Department of Medical Laboratory Science, College of Science, Komar University of Science and Technology (KUST), Qliasan st, 46002 Sulaimaniyah, Kurdistan Region, Iraq*

Received 26 December 2020; accepted 14 February 2021
Available online 24 February 2021

KEYWORDS

Antibacterial;
Antifungal;
Zinc peroxide;
Low-temperature synthesis

Abstract In the present work, a fast, facile, low temperature, and surfactant free synthesis procedure is developed for the preparation of zinc peroxide nanoparticles (ZnO_2NPs) in methanol solution. ZnO_2 were prepared via reduction of methanolic solution of zinc ions using $NaBH_4$ as a reducing agent to metallic zinc, followed by oxidation using hydrogen peroxide. The produced ZnO_2 nanoparticles were characterized using TEM, SEM, TG, DSC, Raman, XRD, FTIR, UV–Vis absorption spectroscopy. The mean size of the nanoparticles was around 15 nm based on SEM and TEM measurements. Interestingly, ZnO_2 showed effective antibacterial and antifungal activities. Antibacterial activity was examined versus medically substantial Multidrug Resistant Bacteria (MDR) Gram-positive, *Methicillin-Resistant Staphylococcus Aureus* (MRSA), and Gram-negative, *klebsiella pneumoniae* (MDR). Low concentration as 16 mg/L was recorded as minimum inhibitory concentration (MIC) towards the MDR bacterial. Antifungal activity was conducted against *Candida albicans* (C. albicans), *and 16 mg/L was measured as MIC*. Thus, low cost and facile preparation strategy for fabrication of ZnO_2 nanoparticles merged with their effective antibiotic activity will open a door for further utilizing this kind of peroxide nanomaterials in other biological applications.

1. Introduction

The emergence and increasing number of multidrug resistance (MDR) bacteria in the recent years has gain scientific attention in the research communities as they pose serious threat to human health. To that aim, synthesis of novel materials with broad spectrum antimicrobial activities for augmenting and/or replacing conventional antibiotics are highly required

* Corresponding authors at: Department of Chemistry, College of Science, University of Sulaimani, Qliasan st, 46002 Sulaimaniyah, Kurdistan Region, Iraq (D.D. Ghafoor).
E-mail address: Khalid.omer@univsul.edu.iq (K.M. Omer).
Peer review under responsibility of King Saud University.

Production and hosting by Elsevier

https://doi.org/10.1016/j.arabjc.2021.103090

(Wang et al., 2017). These drugs are essential in many other medical procedures such as surgeries, immunosuppressive chemotherapy and organ transplantation to reduce the human mortality and morbidity drastically (Marti et al., 2014). Additionally, antibiotics are highly required in other fields, such as dental implantation and orthodontics, interior and exterior of buildings, and household materials (Jayaraman, 2015; Łyczek et al., 2018; Hodgson, 1998).

Antibiotic resistance is occurring through intrinsic effects, mutations in chromosomal genes or horizontal gene transfers (Alekshun and Levy, 2007). Bacteria can reduce the effect of antibiotics by different mechanisms which includes: reduced drug permeability across the bacterial cell wall which causes the reduction of drug efficiency, antibiotic inactivation and the destruction of the drug active components by microbial enzymes, acquisition of alternative metabolic pathways to those inhibited by the drug, creating transport proteins (efflux pumps, EP) in the cytoplasmic membrane which can remove toxic molecules, and overproduction of the target enzyme (Alekshun and Levy, 2007; Giedraitienė et al., 2011; Fernández and Hancock, 2013; Piddock, 2006).

Infection by various bacteria manifest itself as an important cause of morbidity and mortality worldwide. In a 2009 update from the Infectious Diseases Society of America (IDSA) (Boucher, 2009), *Staphylococcus aureus (S. aureus)* along with *Klebsiella pneumoniae* were identified as the pathogens of most current concern. In particular, methicillin resistant *S. aureus* (MRSA) which show rapidly increasing rates of infection (Boucher, 2009). *S. aureusis* colonize the moist squamous epithelium of anterior nares and other skin districts of healthy person. This microorganism can become a versatile pathogen causing a broad spectrum of infections. *S. aureus* ranks second among bacterial pathogens causing bloodstream infections (Biedenbach et al., 2004; Bissell, 2006), and is the leading cause of nosocomial pneumonia (Hoban et al., 2003). On the other hand, Klebsiella pneumoniae causing a wide spectrum of hospital and community-acquired infections. This gram negative bacteria are divided into three phylogroups that differ in their virulence factor contents these includes Klebsiella pneumoniae, *K. variicola,* and *K. quasipneumoniae*. The isolates of the latter two are often misidentified as Klebsiella pneumoniae and are often misidentified for that they are designated as *K. pneumoniae* complex (KPN complex). Isolates of the KPN complex may be found in many environments such as surface water, soil, and plants (Sylvain and Grimont, 2006). *K. pneumoniae* has been identified in a large number of hospitalized patients such as urinary tract infection, pneumonia, bloodstream infection (BSI), meningitis and pyogenic liver abscess (PLA). The mortality in invasive infection is high, ranging between 17.5 and 23%.

C. albicans is an opportunistic pathogenic yeast and the most common cause of genital yeast infections. It is a type from the fungi which causes life-threatening systemic infections asymptomatically colonizes many areas of the body, particularly the gastrointestinal and genitourinary tracts of healthy individuals (Alcazar-Fuoli and Mellado, 2014). *C. albicans* can cause two major types of infections in humans: superficial infections, such as oral or vaginal candidiasis, and life-threatening systemic infections (Calderone and Candida, 2012).

Over the past few years, metal oxide nanoparticles have become an attractive bactericidal agent including oxides of zinc, iron, copper, titanium, silver, and magnesium. For instance, zinc oxide nanoparticles (ZnO NPs) are a promising and popular platform for the biomedical applications such as anticancer, (Lakshmi et al., 2019); antibacterial (Bharathi and Bhuvaneshwari, 2019), antifungal (Journal et al., 2017), anti-inflammatory (Agarwal and Shanmugam, 2019) and antidiabetic activities (Vinotha, 2019). The generation of large number of the reactive oxygen specious (ROS) is the mechanistic route to the antibiotic activity. The safety and stability of ZnO nanoparticles are among the leading reasons behind their wide spread medical applications (Raghunath and Perumal, 2017; Zhao et al., 2015; Samanta, 2017).

Zinc peroxide nanoparticles (ZnO_2 NPs) is inorganic nanoparticles with a broad tremendous application in various fields including physical, chemical, electronic, biomedicine and environmental (Čubová and Čuba, 2020; Gao, 2011; Wolanov et al., 2013; Simanjuntak et al., 2018; Prikhodchenko, 2014; Uppal, 2017). Moreover, it has been reported that ZnO_2 is safe and produce no threat to the human's health (Meleney, 1941).

ZnO_2 nanoparticles have been used for biomedical applications such as anticancer (Elbahri, 2017), antibacterial, antifungal, anti-inflammatory (Ali et al., 2017), and with other nanomaterials, such as carbon dots for some applications such as organic compound degradation and dye removal (Ramírez, 2020; Chen, 2020; El-Shamy, 2020; El-Shamy, 2020). In biomaterials area, ZnO_2 class recently gained much attraction as antimicrobial agent due to its various bioactivities (Fröber et al., 2020).

The mechanism of the action of bioactive nanoparticles is mainly due to the oxidative stress, which releases of Zn^{2+} ions, and the disruption of microbial cell walls (Pasquet, 2014). It was proved that the smaller sizes show more activity comparing to the larger particles, as smaller size have larger surface area in relation to volume and can more easily penetrate into the bacterial walls (Padmavathy and Vijayaraghavan, 2008).

Oxidative stress will increase the ROS production which includes superoxide anion ($O_2^{\cdot-}$), hydrogen peroxide (H_2O_2), hydroxyl radical ($^{\cdot}OH$), and singlet oxygen ($^1O_2$). These highly reactive molecules can impair bacterial amino acids causing oxidation of the amino acids sulfhydryl groups, blocking RNA transcriptions and DNA syntheses, damaging of nucleic acids, peroxidation of lipids, and activation of the programmed cell death pathway and ultimately leading to cell death (Çimşit et al., 2009).

ZnO_2 nanoparticles were prepared using different techniques, such as co-precipitation method (Ali et al., 2017). Synthesis of this nanoparticle using other classic techniques such as hydrothermal synthesis, laser ablation, and sol gel are not suitable for biomedical application as these routes always led to aggregation and polydispersities of the nanoparticles (Li, 2017; Gondal et al., 2010; Sun et al., 2007). Nevertheless, most of the reported methods suffer from using surfactant in the preparation strategy. One should avoid using surfactant especially if practical application is needed.

The aim of this study is to synthesize surfactant free ZnO_2 nanoparticles in the methanol under low-temperature, followed by exploring their antimicrobial properties against different bacteria and fungi. Fig. 1 shows the scheme for preparation of ZnO2 nanoparticles and their applications as pathogenic antibacterial and antifungal. Reduction of zinc ions followed by oxidation of zinc metal were exploited to make nanoparticles of ZnO_2. Antibacterial and antifungal of the ZnO_2-NPs were evaluated and analyzed completely.

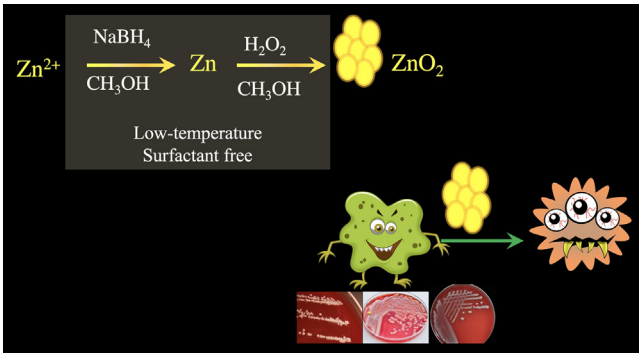

Fig. 1 Scheme for preparation of ZnO_2 nanoparticles and their application against pathogenic bacteria and fungus.

2. Experimental section

2.1. Materials

All chemicals were of the highest purity available and were used as received without further treatment. Zinc acetate dihydrate Zn $(CH_3COO)_2{\cdot}2H_2O$ (98% Aldrich), hydrogen peroxide (30 w/w % Merck), methanol, ethanol, sodium borohydride $NaBH_4$ (98% Aldrich), NaCl (Aldrich > 99%), and double deionized water were used throughout the experiment. All solvents used were of analytical grade and purchased from Aldrich.

2.2. Preparation of zinc peroxide nanoparticles

Room-temperature synthesis method was modified and developed for the synthesis of ZnO_2 nanoparticles. Briefly, 100 ml of 0.01 M zinc acetate dihydrate clear solution was prepared by methanol. 0.075 g sodium borohydride was then added to the solution with continuous stirring for 15 min, then 4.0 ml 15% hydrogen peroxide (H_2O_2) was added to the mixture and stirred continuously for another 15 min. Later on, the solution was put in microwave for one minute (1000 Watts) with continues stirring for 5 min and a pale-yellow suspension solution was produced. This suspension was then centrifuged at 5000 rpm for 10 min, then the precipitate was washed repeatedly by ethanol. The precipitate was dried at 60 °C for 7 h in oven to obtain fine powder.

2.3. Characterization of ZnO_2NPs

The characterization of the ZnO_2 NP crystalline structure was performed by X-ray diffractometer (PAN Analytical Xpert – PRO- XRD) with Cu-Kα radiation (1.54 A_o) and position 2θ values are between (10°–80°) with a step size of 0.1° and a scanning rate of 1 steps/second was employed. The X-rays used for this purposed were generated at 45 kV and 40 mA. Scanning electron microscopy (SEM) with energy dispersive X-ray spectroscopy (EDS) by using (SEM Quanta 200). Transition electron microscopy (TEM) by using (Philips EM208S 100 Kv). Analysis of the thermal behavior of synthetic ZnO_2 NP was done using differential scanning calorimetry (DSC, DSC131 evo) and Perkin Elmer Thermal Analysis (TGA, Diamond TG/DTA) at a heating rate of 10 °C/min under a nitrogen atmosphere. UV–Visible spectrophotometer instrument of (Agilent Technologies Cary 60 UV–Vis Spectrophotometer Model G6860A) was used, the absorption spectra of the NPs were measured in the quartz cuvette with a 1 cm path length. The deionized water was used as a reference material for background correction. FTIR was performed using a (PE IR SPECTRUM ASCII PEDS 1.60 spectrometer) and sample were presented as KBr pellet. Spectra were acquired at room temperature at resolution of 4 cm^{-1}.

2.4. Bacterial strains and reagents

Mueller Hinton agar (MHA) was purchased from Himedia (Himedia, India). Sorbitol Mac Conkey Agar, Lab M is a Neogen company (M Limited, UK) product. Mannitol Salt Phenol Red Agar, from Sigma Aldrich (St. Louis, MO, USA). Sabouraud's dextrose agar (SAD) "Pharmacopoeia, New York, USA". Gram-positive Bacteria (*Methicillin-Resistant Staphylococcus Aureus* (MRSA)), Gram-negative (*klebsiella pneumoniae* MDR), and Fungi *Candida albicans* was isolated and identified at the Medical Laboratory Science Labs.

2.4.1. Identification of microbial pathogens

A total of 3 swabs of bacteria and 1 fungus were isolated from hospitalized patients at Shar Hospital, Sulaimaniyah, Iraq. All 4 pathogens were first confirmed by microbial identification (ID) using the VITEK® 2 automated systems (BioMérieux, Marcy-L'E'toile, France). The swabs were then transferred to the Microbiology Lab at the College of Science, Sulaimani University, Iraq, and immediately inoculated on selective and non-selective culture media. To confirm identification of bacteria, the swabs were cultured on Mannitol Salt Phenol Red Agar, Sorbitol Mac Conkey Agar, and Mueller Hinton agar (MHA) for bacteria, and were inoculated on Sabouraud's dextrose agar for identification of fungi. The plates were incubated under aerobic conditions for up to 20 h for bacteria and 72 h for fungi. Phenotypic identification and conventional biochemical tests for bacteria and fungi were performed (Tang and Stratton, 2006; Pincus, 2010; Sanguinetti, 2007).

2.4.1.1. DNA extraction. The genomic DNA was extracted from all isolates using an AmpliSens nucleic acid extraction Kit (AmpliSens® DNA-sorb-AM, USA). The bacterial isolate was first grown on nutrient broth media for 24 h at 37 °C in an incubator. The bacterial isolate was incubated at 37 °C for 24 h to grow on nutrient broth media and then 1.5 ml of the liquid culture was added to a 1.5 ml microcentrifuge tube. The tubes were centrifuged at 13000 rpm for 2 min to pellet the cells. 300 µl of the lysis solution was added and then the samples were vortexed for homogenization. The samples were incubated at 65 °C for 5 min and 400 µl precipitate solution was added to all samples then tubes were centrifuged at 13000 rpm for 5 min. Finally, the samples were washed with 500 µl washing solution and 200 µl of washing buffer. The supernatant was then discarded and the pellet was dried at 65 °Cfor 5 min then 50 µl of RNA buffer were added to make DNA solution. The extraction of cellular DNA was done according to the protocol provided by AmpliSens nucleic acid extraction Kit. The extracted DNA was stored at 4 °C for further work. The extracted DNA was quantified by spectrophotometric measurement at a wavelength of 260 nm according to

the method described by Sambrook and Russell (Lucena-aguilar et al., 2016).

The 16S rRNA genes were selectively amplified from purified genomic DNA by using oligonucleotide primers designed to anneal to conserved positions in the 3′ and 5′ regions of bacterial 16S rRNA genes. The forward primer and the reverse primers and the PCR conditions are shown in Tables 1 and 2, respectively.

The reaction conditions were as follows: using master mix kit HS Prime Taq Premix (2X) (GenNet Bio) which contain HS Prime Taq DNA polymerase 1unit/10 µl, 2X reaction buffer, 4 mM $MgCl_2$, sediment, loading dye, pH 9.0 and 0.5 mM each of dATP, dCTP, dGTP, dTTP and add 7 µl deionized water and 1 µl of each forward and reverse primer. Amplification was carried out in 200 µl tubes in a PTC-1000 thermal cycler (Bio-RAD) as shown in Tables 2 and 3:

2.4.1.2. Detection of DNA using agarose gel electrophoresis. After PCR reaction, the product was checked using horizontal gel electrophoresis in 1.0% agarose slab gel in Tris–borate EDTA (TBE) buffer. Agarose was first dissolved in 1X TBE buffer and was heated to dissolve in a microwave oven for about 30 s. After cooling the agarose solution to around 50 °C, 2 µl Ethidium Bromide (EtBr) stain was added and mixed in order to stain the DNA bands. The agarose was then poured on the tray previously set with the comb and allowed to solidify. The combs were removed and 6 µl aliquot of the PCR product was mixed 2 µl of loading dye and was loaded into the individual wells of the gel. A ladder of size 1 kb plus (Invitrogen, USA) was used to ensure amplification of the desired gene and measure the exact product size which was estimated to be within 1,500 bp. The DNA bands were observed on a UV transilluminator at 365 nm.

2.4.1.3. Measurement of DNA concentration and purity. The DNA quantity and the purity of extracted DNA were determined by a NanoDrop instrument (Nanodrop 1000 Spectrophotometer Thermo Scientific) at 260 nm. To the NanoDrop, 1.5 µl of nuclease free water was used as blank. The blank was removed and 1.5 µl of sample was loaded. By using 10 µl DNA extracted solution mixed with 90 µl of distilled water. DNA concentration was measured in ng/µl unit.

2.4.1.4. DNA sequencing. DNA sequencing was found using Sanger method.

2.4.1.5. Bioinformatics analysis. The acquired gene sequence trace was trimmed and cleaned using Mega6 and Lasergene Seqman software. The cleaned genetic sequence was then compared to different 16S rRNA gene of different bacteria in the reference RNA sequences (16S ribosomal RNA) database of NCBI Nucleotide BLAST website using Blast tool in order to identify the genus of the selected isolate.

The query sequence was converted to FASTA format.

Table 1 Forward and reverse primers for amplification of the microbial genes.

Primers code	primers name
AGAGTTTGATCMTGGCTCAG	27f universal
GGTTACCTTGTTACGACTT	1492r
TCCGTAGGTGAACCTGCGG	ITS1 candida
TCCTCCGCTTATTGATATGC	ITS4

Table 2 PCR reaction condition Temperature protocol of (27F, 1492R) and (ITS1, ITS4) primers.

Number of cycles	Stage name	execution time	Temperature (° C)
1	Primary degeneration	5 min	95
	Degeneration	30 sec	95
15	Connection	30 sec	60
	Expansion	30 sec	72
1	Final expansion	10 min	72

2.5. Bacteria susceptibility test for define MDR strains

Antibiotic susceptibility testing was performed by disc diffusion method by the Clinical and Laboratory Standards Institute (CLSI) for bacteria and yeasts testing and Kirby-Bauer method (Walker, 1999). Agar plates of Muller-Hinton was prepared. For inoculum preparation, the bacterial isolates were inoculated on nutrient broth separately and incubated at 37 °C. The suspension was then vortexed and diluted in normal saline to adjust the bacterial concentration at turbidity equivalent to that of 0.5 McFarland standards or 1×10^8 colony-forming units (CFUs)/mL and was then spread on MHA agar to grow. Sixteen Antibiotic discs namely ampicillin (AMP), amoxicillin (AX), aztreonam (ATM), ciprofloxacin (CIP), cefoxitin (FOX), ceftazidime (CAZ), cefotaxime (CTX), gentamicin (GEN), imipenem (IMP), Keflex (cephalexin) (KF), meropenem (MEM), nitrofurantoin (F), nalidixic acid (NA), ticarcillin (TC), tobramycin (TOB), and methicillin (M) were immediately placed on the surface of the agar plate using forceps, left for 15 min at room temperature for diffusion and incubated aerobically at 37 °C for 16 h. Inhibition zones for various isolates were measured and interpreted as sensitive, intermediate, or resistant according to the Clinical Laboratory Standards Institute (CLSI) (Walker, 1999). MDR was defined as resistance to at least 3 or more antimicrobial categories.

2.6. Determination of antimicrobial activity

2.6.1. Antibacterial activity

The antimicrobial effect of ZnO_2 NPs was studied versus both gram- positive and gram-negative with multidrug resistant (MDR). *Methicillin-Resistant Staphylococcus Aureus* (*MRSA*) as the gram- positive organism, and for gram-negative *klebsiella pneumoniae* MDR, was used. Minimum inhibitory concentrations (MIC) which is defined as the lowest concentration of the assayed antimicrobial agent that inhibits the visible growth of the microorganism tested was determined using microplate reader (Biotek). Minimal bactericidal Concentration (MBC) values were determined after (MIC values) which offers the possibility to quantitatively estimate the lethality concentration of the tested antimicrobial agent in the broth (Balouiri et al., 2016). For the aforementioned purposes, Broth Microdilution method was trailed.

Table 3 Comparative data to blast in NCBI.

	Top-hit taxon	Top-hit strain	Similarity (%)	Top-hit taxonomy	Completeness (%)
A	Staphylococcus aureus	**S33 R**	**100.00**	cellular organisms; Bacteria; Terrabacteria group; Firmicutes; Bacilli; Bacillales; Staphylococcaceae; Staphylococcus; Staphylococcus aureus.	**95.7**
B	Klebsiella pneumoniae	**DSM 30104**	**99.22**	Bacteria; Proteobacteria; Gammaproteobacteria; Enterobacterales; Enterobacteriaceae; Klebsiella	**96.4**
C	Klebsiella pneumoniae	**ATCC 13883**	**99.02**	Bacteria; Proteobacteria; Gammaproteobacteria; Enterobacterales; Enterobacteriaceae; Klebsiella.	**96.1**
D	Candida albicans strain H294A	**KP675005.1**	**100.0**	Eukaryota; Fungi; Dikarya; Ascomycota; Saccharomycotina; Saccharomycetes; Saccharomycetales; Debaryomycetaceae; Candida/Lodderomyces clade; Candida	**95.2**

2.6.1.1. Broth microdilution method. To determine the minimum inhibitory concentrations (MIC) of ZnO_2 NPs in own solution, bacterial strains were cultured in Mueller Hinton Broth (MHB). Cell suspensions were adjusted to obtain standardized populations by measuring the turbidity with a spectrophotometer (Agilent Technologies Cary 60 UV–Vis Spectrophotometer Model G6860A). Susceptibility tests were performed by two fold microdilution of the ZnO_2 in standard broth following the Clinical and Laboratory Standards Institute (CLSI) guidelines (CLSI, 2015). The bacterial strains, at (1×10^6 cell /ml), were inoculated into MHB, and 0.1 ml was dispensed per well into a 96-well microtiter plate. *klebsiella pneumoniae* (DSM 30104), *klebsiella pneumoniae* (ATCC 13883) and Methicillin-Resistant *Staphylococcus Aureus* (MRSA) were then exposed to 0.1 ml of different concentrations (1, 2, 4, 8, 16, and 32) mg/mL of ZnO_2 NPs (which stock solution diluted by Mueller Hinton broth (MHB). Growth after 24 h of incubation was assayed using a microplate reader (The Biotech EL800 Microplate Reader, USA) by reading absorbance at 630 nm, the results showed in Table 1. And for MBC after read by microplate reader, on Mueller Hinton agar (MHA) cultured 0.01 ml of each well which contain different concentrations of ZnO_2 NPs treated with bacteria were incubated for 24 h to determine lethal concentration.

2.6.2. Antifungal activity

The antifungal activity of ZnO_2 nanoparticles was evaluated against phytopathogenic fungi; C*andida albican* using poisoned food method and well diffusion method.

2.6.2.1. Poisoned food method. The test done according to (Balouiri et al., 2016; Balouiri et al., 2016) with slight changes. Briefly, ZnO_2 particles were mixed with Sabouraud Dextrose Agar (SDA) medium at the concentrations of 0, 1, 2, 4, 8, 16, 32 and 64 Mg/mL of ZnO_2 particles, and deionized water was used as a control. After that, 0.1 ml of freshly-grown spore suspension sample (1×10^6 CFU/mL) was inoculated at the surface of the SDA plates. The antifungal experiments were carried out as triplicates. Each inoculated SDA plate was incubated at 29 ± 1 °C for 6 days in darkness. Record the MIC as the lowest concentration of antimicrobial agent that completely inhibits growth, recorded at the end of the incubation period Table 2.

2.6.2.2. Well diffusion method. The well diffusion test (Magaldi, 2004) was favorited work with (GMB) Medium (M44-A. 2004) (Mueller-Hinton Agar + 2% Glucose and 0.5 µg/mL Methylene Blue Dye). Briefly, The density of conidia in the spore suspension was optically adjusted, after swabbing of (10^6 cells/mL) number of fungal cells with the sterile cotton swab on to the surface of the agar plate, then they will allowed to dry for 10 min, followed by punching four wells of 7 mm diameter into GMB agar and filled with 100 µl of different concentrations 50, 100, 150 and 200 Mg/mL of ZnO_2 particles (which prepared from dilution stock solution with MHB), and two antifungals drug (Clotrimazole 10 mg/L and Fluconazole 40 mg/L) (for compression). The antifungal drug (Fluconazole and Clotrimazole) purchase from Pioneer Pharmaceutical Company, Sulaimaniyah, Iraq by a pure powder form. Incubate agar plates at 35 °C for 24 h. After that recorded clear zone inhibition for vision the Anti-Candida activity Table 5 and Fig. 4II.

3. Results and discussion

3.1. Chemical structure, size and morphology

X-ray diffraction spectrum was used to examine the crystalline forms, known as 'phases' of compound present in powder and solid samples. Fig. 2A shows the XRD pattern of crystalline ZnO_2 nanoparticles. As one can notice the spectrum is noisy and broad assigning for the nature of the prepared ZnO_2 nanoparticles. They crystalline ZnO_2 nanoparticles, displayed four broad peaks at $2\theta = 31°, 36.5°, 53°, 63°$, corresponds to (1 1 0), (2 0 0), (2 2 0), (3 1 1), planes of ZnO_2 respectively, which confirmed that the prepared sample was cubic crystal ZnO_2 NPs (Bergs, 2017; Zn, 2014).

Further broadened respect could be detected for samples indicating the presence of nanoparticles (Kurapati et al., 2016). By measuring the full width at half maximum (FWHM) of the (1 1 0), (2 0 0), 220 and 311 it was possible to calculate the crystallite sizes of the samples via the well-known Debye Scherer equation. The ZnO_2 NP are in the nanometer range as it is proved by the broadening of the XRD reflections and the average crystallite size NPs was about 24 nm as calculated by the Scherer's equation: $D = k.\lambda/(\beta.\cos\theta)$, where $k = 0.9$; λ is the wavelength of monochromatic X-ray radiation

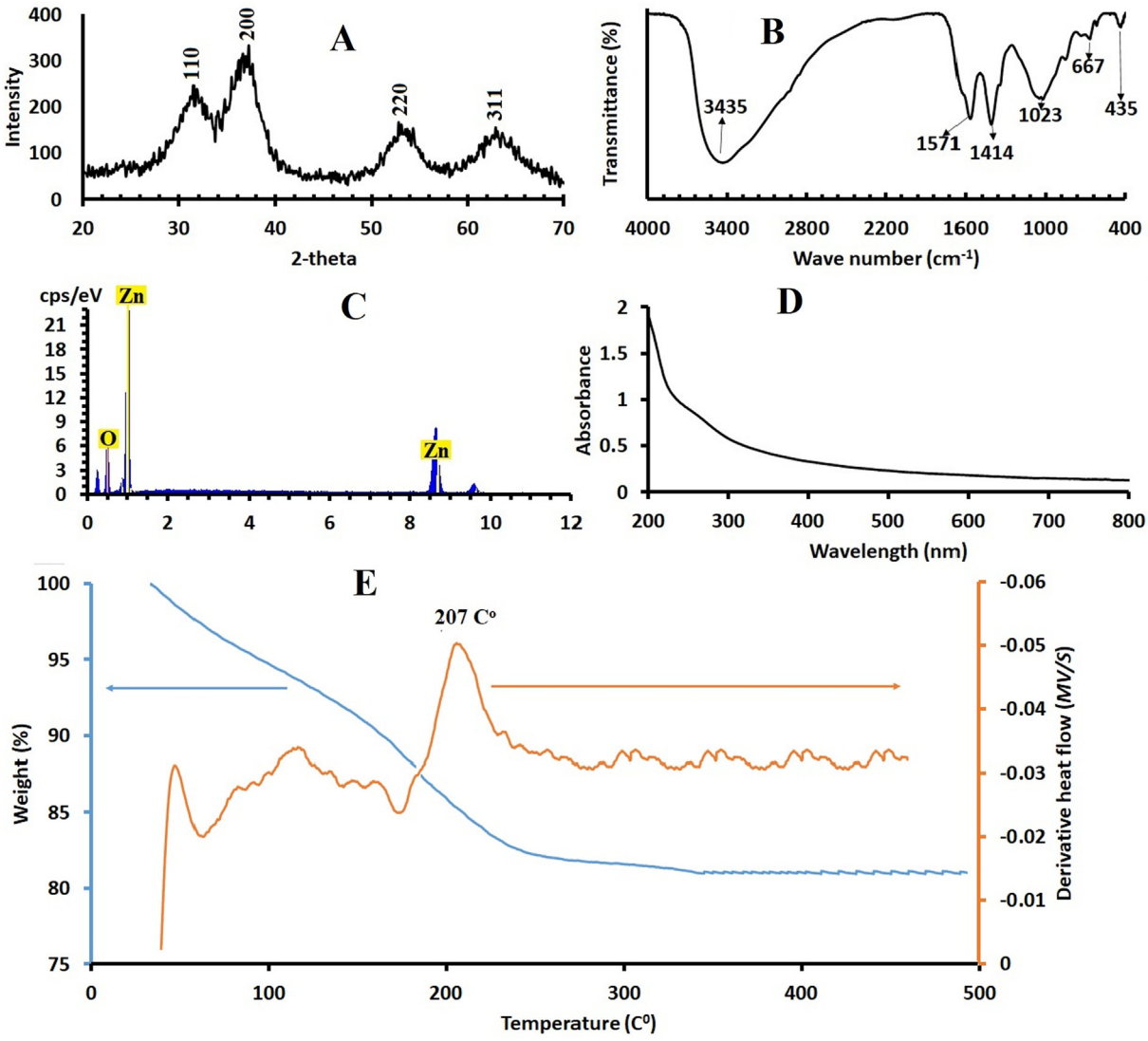

Fig. 2 **A**. The XRD of ZnO_2 NPS. **B**. FTIR spectra of ZnO_2 nanoparticles **C**. EDX for ZnO_2.. **C**. UV–visible absorption spectrum of synthesized ZnO_2 NPs. **E**. Thermogravimetric analysis (blue solid line) and differential scanning calorimetric curves (brown line) of the synthetic ZnO_2 -NPs.

(λ = 1.5406 Å), θ is the Bragg, angle and β is the full width of X-ray pattern line at half peak.

The FTIR spectra of ZnO_2 nanoparticles were recorded (Fig. 2b). To identify the functional groups present on ZnO_2 nanoparticles. A broad absorption peak at 3300–3800 cm^{-1} is attributed to stretching mode of hydroxyl groups (O—H). Several other characteristic peaks at 667 cm^{-1}, 1023 cm^{-1}, 1414 cm^{-1} and 1571 cm^{-1}. Absorption peaks at 667 cm^{-1}, 1023 cm^{-1} and 1414 cm^{-1} may be due to the O—O bands corresponding to the peroxide (O_2^-) ions of ZnO_2 nanoparticles. 437 cm^{-1} is related to Zn—O characteristic vibrations. The FTIR peaks confirms presence of functional groups on the surface of ZnO_2 and also formation of ZnO_2 nanoparticle FT-IR spectrum does not show any of absorption bands of —COO or —CH_3 groups of zinc acetate, suggesting the purity of synthetic ZnO_2 -NPs and does not show any of absorption bands of —COO or —CH_3 groups of zinc acetate, suggesting the purity of synthetic ZnO_2 -NPs (Aguilar et al., 2011; Cheng et al., 2009).

In Fig. 2C the typical EDX spectrum of ZnO_2 is shown. This indicates the composition of the sample which is formed by Zn and O (the atomic ratio Zn/O is 1:2.1), approaching that of the consulted bibliography, supporting the approximated chemical composition that could be estimated for ZnO_2 according to the obtained XRD results.

4. Optical and thermal properties

The optical study of the ZnO_2-NPs was performed via measuring the absorbance of ZnO_2 nanoparticles s shown in Fig. 2D ZnO_2 showed a peak below 300 nm, absorbance spectra for ZnO_2 which is located at 272 nm, similar absorption spectra were reported in literature (Ramírez, 2020; Moller, 2019).

The Thermal stability and thermal-induced transformation of ZnO_2 to ZnO have been studied and shown in the TGA and DSC curves Fig. 2E, the results revealed the thermal behavior of synthetic ZnO_2 from room temperature, 25 °C up to 500 °C.

The TGA curve shows weight losses in temperatures ranging from 33 °C to 500 °C; about 11% mass loss of below 100 °C, corresponding to the loss of water, methanol and ethanol adsorbed on the surface of the ZnO_2 particles. This was also confirmed by the DSC curves showing endothermic peak at 75 °C. Another region shows a 12.6% second mass loss ranging from 165 °C to 245 °C which is attributed to the oxygen molecule loss. Oxygen loss is based on the reaction: $2ZnO_2 \rightarrow 2ZnO + O_2$ and the remaining is ZnO which is almost constant up to 500 °C as shown in XRD spectrum. The DSC curve revealed an exothermic peak at 207 °C that is in agreement with abrupt weight loss in TGA curve.

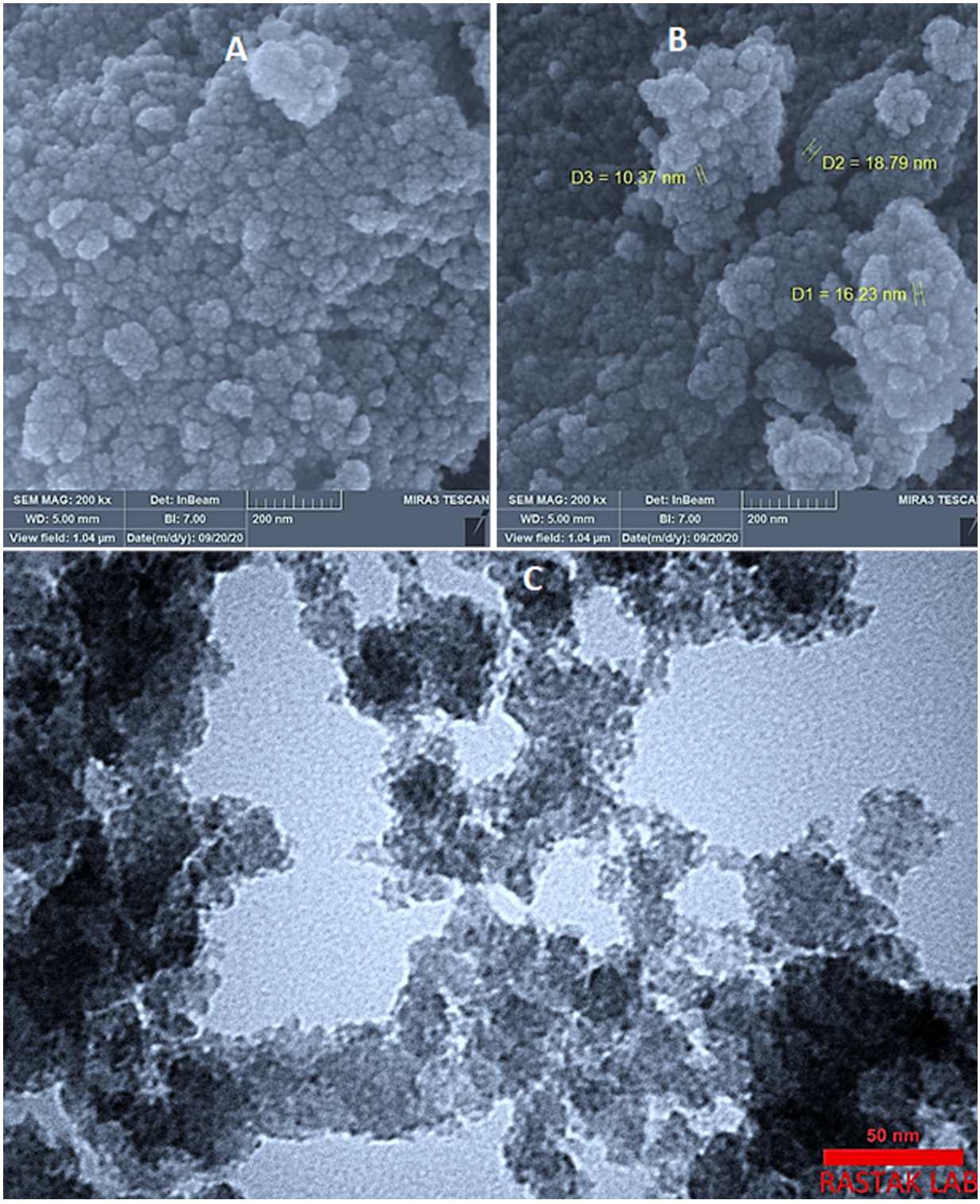

Fig. 3 A and B) SEM images of ZnO_2-NPs, the images were taken under 100 KV. C) TEM image of ZnO_2-NPs, applied voltage: 300 KV.

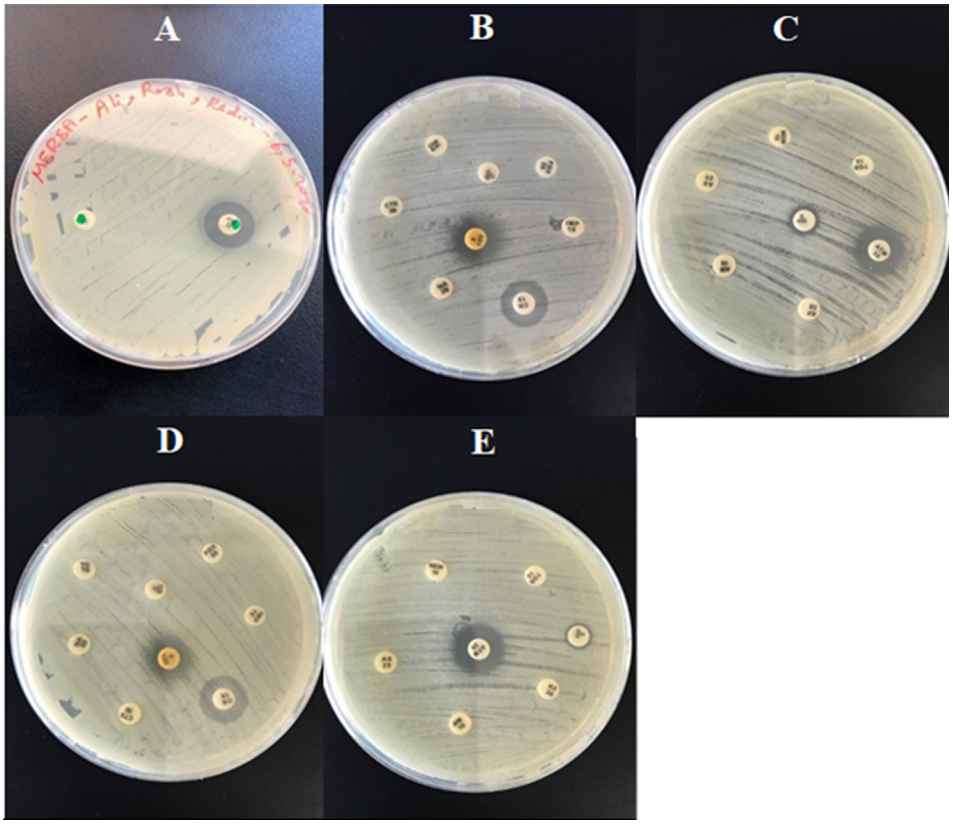

Fig. 4 A. MRSA vs methicillin and cefoxitin Antibiotic disk. B, C, D, and E are two type Klebsiella pneumoniae (DSM 30104, ATCC 13883) vs all Antibiotic disk that used except methicillin.

Table 4 Determination of MIC value of ZnO_2 NPs (concentration of ZnO_2 NPs by *m*g/ml).

Microbials species	MIC value (conc. of ZnO_2 NPs by mg/L)
S. Aureus MRSA	16
klebsiella pneumoniae DSM 30104	16
klebsiella pneumoniae ATCC 13883	16

SEM images of synthetic ZnO_2 -NPs was showed in Fig. 3A and B. The nanoparticles are well dispersed and non-agglomerated in water medium. Moreover, spherical and boundary of individual particles can be noticed. The average particle sizes are in the range of 10–20 nm which is very close to the crystallite size calculated from XRD results.

The TEM images of ZnO_2 nanoparticles is shown in Fig. 3C and it demonstrates the possibility of precise determination of spherical ZnO_2-NPs. The results indicate that synthetic ZnO_2-NPs have well-dispersed ZnO_2 –NPs and they are spherical.

4.1. Genotypic characterization of the bacteria and fungi

The concentration of the DNA extracted has been obtained and it was fit for phylogenic analysis as the quality of purification is close to 2.0 and DNA concentrations were between 150 and 185 ng/ ml. The phenotypic observation of *klebsiellas*, *S. aureias*, and *C. albicans* checked genotypic by using 16 s rRNA sequencing which is shown in supplementary file. The result of 16 s rRNA when blast in NCBI shown in Table 3.

4.2. Sensitivity testing for microbial strains

The susceptibility of *klebsiellas* and *S. aureaus* to commercial 15 antibiotic agents was determined. The intermediate sensitivity of 2 *klebsiella*'s against GEN and show resistant for 14 antibiotics. And *S. aureaus* show resistance again methicillin and FOX antibiotic. The results are shown in Fig. 4.

4.3. Antimicrobial activity of ZnO_2 -NPs against MDR strains

There are fewer reports that have investigated antibacterial and antifungal activities of ZnO_2 NPs (Ali et al., 2017; Fröber et al., 2020; Ali, 2020). Our studies have been conducted to investigate ZnO_2 -NPs against polymicrobial MDR. Antibacterial activity was examined versus medically substantial Multidrug Resistant (MDR) Bacteria Gram-positive (*Methicillin-Resistant Staphylococcus Aureus* (MRSA)) and Gram-negative (*klebsiella pneumoniae* MDR) Table 4 and Fig. 5I. Antifungal activity was conducted against *Candida albicans (*C. albicans*)* Table 5, Fig. 5II, and Fig. 5III.

The ZnO_2-NPs showed significant inhibitory activity against the strains tested with distinct differences in the susceptibility to ZnO_2-NPs in a dose-dependent manner. Both of

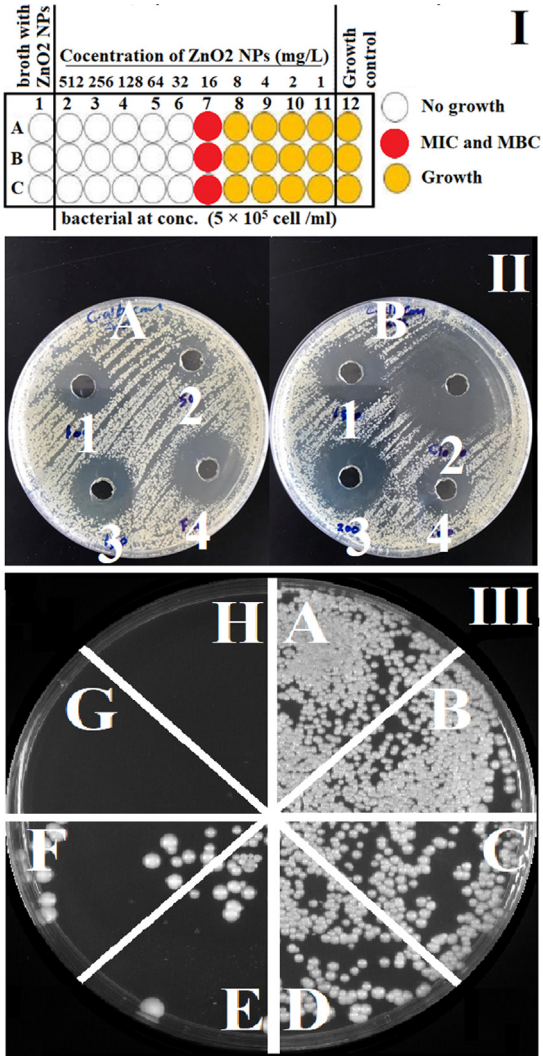

Fig. 5 Antimicrobial activity of ZnO_2 NPs **I.** Anti-Bacterial activity by broth microdilution method for ZnO_2-NPs a gain: A. *Staphylococcus Aureus* (MRSA). B and C are Klebsiella pneumoniae (DSM 30104, ATCC 13883). It shows the MIC and MBC for all three bacteria equal to 16 mg/L of ZnO_2-NPs. **II.** Antifungal activity of ZnO_2 NPs and two antifungal drug a gains *C. albicans* by well diffusion method. **A**. 1, 2, 3 and 4 They represent (100, 50, 150) *mg/L* ZnO_2 and 40 *mg/L* Fluconazole respectively. **B.** 1, 3, 4 They represent (150, 100, 200) *mg/L* ZnO_2 respectively and 2 is a 10 *mg/L* Clotrimazole. **III.** Anti-fungal activity for ZnO_2 NPs a gains candida albican by using agar dilution method. **a.** *Candida albicans* (C. albicans), b, c, d, e, f, g and h are C. albicans with *1, 2, 4, 8, 16,* 32 and 64 *mg/L* ZnO_2 respectively. It shows the lethal concentration of ZnO_2-NPs which required for killing completely *C. albicans* is 16 mg/L.

MIC and MBC were equal to 16 mg/mL for the bacteria. High efficiency of ZnO_2-NPs as antifungal illustrated which 16 mg/mL for C. albicans fungi strains were found to be the same susceptible as a strains bacteria, and as comparison clear zone inhibition diameter (14, 19, 22, 25) mm of 50, 100, 150, 200 mg/mL for it by zone inhibition diameter (25, 35) mm of Fluconazole 40 mg/mL and Clotrimazole 10 mg/mL respectively. The MIC and MBC are against *Methicillin-Resistant Staphylococcus Aureus* (MRSA) and two strains of *klebsiella pneumoniae* MDR approximately have a same value.

Table 5 MIC of antifungal activity of ZnO_2 NPs and two antifungal drug a gains *C. albicans* by well diffusion method accounting clear zone inhibition diameter.

Antifungals	Clear zone inhibition (by mm) with well.
ZnO_2 NPs 50 mg/L	14
ZnO_2 NPs 100 mg/L	19
ZnO_2 NPs 150 mg/L	22
ZnO_2 NPs 200 mg/L	25
Clotrimazole 10 mg/L	35
Fluconazole 40 mg/L	25

The antimicrobial activities of nanoparticles against bacteria and fungi pathogens depend on particle size, the concentration of the powder, morphology, and specific surface area (Sánchez-López, 2020). Concentration effect on the antibiotic activities has been conducted and the results indicated that the increase in ZnO_2-NPs concentrations (1, 2, 4, 8, 16, 32 and 64 mg/mL) correlated with increasing antimicrobial activities as showed in Fig. 4. This may be attributed to the increased H_2O_2 concentration from the surface of ZnO_2. It can be assumed that the generated H_2O_2 can penetrate the cell membranes of bacteria and fungi that used in this experiment, and kill them. The small particle size of NPs is associated with a larger band gap; consequently, these unfavorable conditions can prevent the recombination of excitons. Therefore, more available and stable excitons will result in the formation of higher concentration of reactive oxygen species, and consequently enhance the antimicrobial activities of metal oxide NPs (Raghunath and Perumal, 2017).

5. Conclusion

In summary, nanobiotechnology has become as an efficient technology for the fabrication and development of antimicrobial materials through simple and eco-friendly approach. Our results showed that ZnO_2 nanoparticles were prepared via simple, surfactant free, lower temperature method, and eco-friendly procedure. The nanoparticles were thermally stable under ambient temperature. Our experimental results displayed the high antibacterial effect of the as-prepared ZnO_2 against multi-resistant bacteria and antifungal pathogen. 16 mg/mL as MIC was reordered towards both pathogenic bacteria and fungus. Stability and easy-production of ZnO2 nanoparticles will contribute to improve the quality of nano-based synthetic antimicrobials.

Declaration of Competing Interest

The authors declare that they have no known competing financial interests or personal relationships that could have appeared to influence the work reported in this paper.

Acknowledgment

Authors thank the University of Sulaimani for opportunity to conduct this research. Hawkar M. Hussain thanks the Min-

istry of Health and Directorate of Health-Sulaymaniyah for the study leave.

References

Agarwal, H., Shanmugam, V., 2019. A review on anti-inflammatory activity of green synthesized Zinc Oxide nanoparticle: Mechanism-based approach. Bioorganic Chem. (Elsevier Inc., 2019). doi: 10.1016/j.bioorg.2019.103423.

Aguilar, A., Rubio-rosas, E., Pe, R., 2011. Structural and vibrational properties of hydrothermally grown ZnO2 nanoparticles. 316, 37–41.

Alcazar-Fuoli, L., Mellado, E., 2014. Current status of antifungal resistance and its impact on clinical practice. Br. J. Haematol. 166, 471–484.

Alekshun, M.N., Levy, S.B., 2007. Molecular mechanisms of antibacterial multidrug resistance. Cell 128, 1037–1050.

Ali, S.S. et al, 2020. Molecular characterization of virulence and drug resistance genes-producing Escherichia coli isolated from chicken meat: Metal oxide nanoparticles as novel antibacterial agents. Microb. Pathog. 143, 104164.

Ali, S.S., Morsy, R., El-Zawawy, N.A., Fareed, M.F., Bedaiwy, M.Y., 2017. Synthesized zinc peroxide nanoparticles (ZnO2-NPs): A novel antimicrobial, anti-elastase, anti-keratinase, and anti-inflammatory approach toward polymicrobial burn wounds. Int. J. Nanomedicine 12, 6059–6073.

Balouiri, M., Sadiki, M., Ibnsouda, S.K., 2016. Methods for in vitro evaluating antimicrobial activity: A review. J. Pharm. Anal. 6, 71–79.

Bergs, C. et al, 2017. Biofunctionalized zinc peroxide (ZnO2) nanoparticles as active oxygen sources and antibacterial agents. RSC Adv. 7, 38998–39010.

Bharathi, D., Bhuvaneshwari, V., 2019. Synthesis of zinc oxide nanoparticles (ZnO NPs) using pure bioflavonoid Rutin and their biomedical applications: antibacterial, antioxidant and cytotoxic activities. Res. Chem. Intermed. https://doi.org/10.1007/s11164-018-03717-9.

Biedenbach, D.J., Moet, G.J., Jones, R.N., 2004. Occurrence and antimicrobial resistance pattern comparisons among bloodstream infection isolates from the SENTRY Antimicrobial Surveillance Program (1997–2002). Diagn. Microbiol. Infect. Dis. 50, 59–69.

Bissell, M.G., 2006. Nosocomial bloodstream infections in US hospitals: analysis of 24,179 cases from a prospective nationwide surveillance study. Yearb. Pathol. Lab. Med. 2006, 285–286.

Boucher, H.W. et al, 2009. Bad bugs, no drugs: No ESKAPE! An update from the Infectious Diseases Society of America. Clin. Infect. Dis. 48, 1–12.

Calderone, R.A.C.C, 2012. Candida and Candidiasis. ASM Press, 2012.

Chen, P. et al, 2020. Facile one-pot fabrication of ZnO2 particles for the efficient Fenton-like degradation of tetracycline. J. Alloys Compd. 834.

Cheng, S., et al., 2009. Soft-template synthesis and characterization of ZnO2 and ZnO hollow spheres, pp. 13630–13635.

Çimşit, M., Uzun, G., Yildiz, Ş., 2009. Hyperbaric oxygen therapy as an anti-infective agent. Expert Rev. Anti. Infect. Ther. 7, 1015–1026.

CLSI, 2015. M07-A10: Methods for dilution antimicrobial susceptibility tests for bacteria that grow aerobically.

Čubová, K., Čuba, V., 2020. Synthesis of inorganic nanoparticles by ionizing radiation – a review. Radiat. Phys. Chem. 169, 108774.

Elbahri, M. et al, 2017. Underwater Leidenfrost nanochemistry for creation of size-tailored zinc peroxide cancer nanotherapeutics. Nat. Commun. 8, 1–10.

El-Shamy, A.G., 2020. An efficient removal of methylene blue dye by adsorption onto carbon dot @ zinc peroxide embedded poly vinyl alcohol (PVA/CZnO2) nano-composite: A novel Reusable adsorbent. Polymer (Guildf). 202, 122565.

El-Shamy, A., 2020. gamal. New carbon quantum dots nano-particles decorated zinc peroxide (Cdots/ZnO2) nano-composite with superior photocatalytic efficiency for removal of different dyes under UV-A light. Synth. Met. 267, 116472.

Fernández, L., Hancock, R.E.W., 2013. Erratum to Adaptive and mutational resistance: Role of porins and efflux pumps in drug resistance (Clinical Microbiology Reviews, (2012), 25, 4, (661–681)). Clin. Microbiol. Rev. 26, 163.

Fröber, K., Bergs, C., Pich, A., Conrads, G., 2020. Biofunctionalized zinc peroxide nanoparticles inhibit peri-implantitis associated anaerobes and Aggregatibacter actinomycetemcomitans pH-dependent. Anaerobe 62.

Gao, D. et al, 2011. Ferromagnetism induced by oxygen vacancies in zinc peroxide nanoparticles. J. Phys. Chem. C 115, 16405–16410.

Giedraitienė, A., Vitkauskienė, A., Naginienė, R., Pavilonis, A., 2011. Correspondence to Antibiotic Resistance Mechanisms of Clinically Important Bacteria. Rev. Med. 47, 137–183.

Gondal, M.A., Drmosh, Q.A., Saleh, T.A., 2010. Effect of post-annealing temperature on structural and optical properties of nano-ZnO synthesised from ZnO2 by laser ablation method. Int. J. Nanoparticles 3, 257–266.

Hoban, D.J., Biedenbach, D.J., Mutnick, A.H., Jones, R.N., 2003. Pathogen of occurrence and susceptibility patterns associated with pneumonia in hospitalized patients in North America: Results of the SENTRY Antimicrobial Surveillance Study (2000). Diagn. Microbiol. Infect. Dis. 45, 279–285.

Hodgson, Michael J., Morey, Philip, Leung, Wing-Yan, Morrow, Lisa, Miller, David, Jarvis, Bruce B., Robbins, Howard, Halsey, John F., Storey M., Eileen, 1998. Building-associated pulmonary disease from exposure to Stachybotrys chartarum and Aspergillus versicolor. J. Occup. Environ. Med. 40, 241–249.

Jayaraman, S., 2015. Interventions for replacing missing teeth: Antibiotics in dental implant placement to prevent complications: Evidence summary of Cochrane review. J. Indian Prosthodont. Soc. 15, 179–182.

Journal, A.I., Padalia, H., Chanda, S., 2017. Characterization, antifungal and cytotoxic evaluation of green synthesized zinc oxide nanoparticles using Ziziphus nummularia leaf extract. Artif. Cells, Nanomedicine, Biotechnol., 1751–1761

Kurapati, R., Vaidyanathan, M., Raichur, A.M., 2016. Synergistic photothermal antimicrobial therapy using graphene oxide/polymer composite layer-by-layer thin films. RSC Adv. 6, 39852–39860.

Lakshmi, R., Pammi, S.V.N., Vijay, P.P.N., 2019. Antibiotic potentiation and anti-cancer competence through bio-mediated ZnO nanoparticles. Mater. Sci. Eng. C 103.

Li, C.Y. et al, 2017. Preparation of tradescantia pallida-mediated zinc oxide nanoparticles and their activity against cervical cancer cell lines. Trop. J. Pharm. Res. 16, 494–500.

Lucena-aguilar, G., Marı, A., Barbera, C., Carrillo-a, A., Lo, A., 2016. DNA source selection for downstream applications based on DNA quality indicators analysis. 00, 1–7.

Łyczek, J., Kawala, B., Antoszewska-Smith, J., 2018. Influence of antibiotic prophylaxis on the stability of orthodontic microimplants: A pilot randomized controlled trial. Am. J. Orthod. Dentofac. Orthop. 153, 621–631.

M44-A. 2004. Method for Antifungal Disk Diffusion Susceptibility Testing of Yeasts; Approved Guideline. NCCLS 24.

Magaldi, S., et al., 2004. Well diffusion for antifungal susceptibility testing. 39–45 doi: 10.1016/j.ijid.2003.03.002.

Marti, E., Variatza, E., Balcazar, J.L., 2014. The role of aquatic ecosystems as reservoirs of antibiotic resistance. Trends Microbiol. 22, 36–41.

Meleney, F.L., 1941. Zinc peroxide in surgical infections. Am. J. Nurs. 41, 645.

Moller, J.A.D., 2019. Structure and optical properties of ZnO and ZnO2. Nanoparticles 56, 49–62.

Padmavathy, N., Vijayaraghavan, R., 2008. Enhanced bioactivity of ZnO nanoparticles - An antimicrobial study. Sci. Technol. Adv. Mater. 9.

Pasquet, J. et al, 2014. The contribution of zinc ions to the antimicrobial activity of zinc oxide. Colloids Surfaces A Physicochem. Eng. Asp. 457, 263–274.

Laura, J.V., 2006. Piddock. Multidrug Resistance Efflux Pumps in Bacteria\n. Clin. Microbiol. 19, 382–402.

Pincus, D.H., 2010. Microbial identification using the bioMérieux VITEK® 2 system. Encycl. Rapid Microbiol. Methods 1–32.

Prikhodchenko, P.V. et al, 2014. Renewable zinc dioxide nanoparticles and coatings. Mater. Lett. 116, 282–285.

Raghunath, A., Perumal, E., 2017. Metal oxide nanoparticles as antimicrobial agents: a promise for the future. Int. J. Antimicrob. Agents 49, 137–152.

Ramírez, J.I.D.L. et al, 2020. Synthesis and characterization of zinc peroxide nanoparticles for the photodegradation of nitrobenzene assisted by UV-light. Catalysts 10, 1–17.

Samanta, P.K., 2017. Review on wet chemical growth and antibacterial activity of zinc oxide nanostructures. J. Tissue Sci. Eng. 08, 8–11.

Sánchez-López, E. et al, 2020. Metal-based nanoparticles as antimicrobial agents: An overview. Nanomaterials 10, 1–43.

Sanguinetti, M. et al, 2007. Evaluation of VITEK 2 and RapID Yeast plus systems for yeast species identification: Experience at a large clinical microbiology laboratory. J. Clin. Microbiol. 45, 1343–1346.

Simanjuntak, F.M., Chandrasekaran, S., Lin, C.C., Tseng, T.Y., 2018. Switching failure mechanism in zinc peroxide-based programmable metallization cell. Nanoscale Res. Lett. 13.

Sun, M., Hao, W., Wang, C., Wang, T., 2007. A simple and green approach for preparation of ZnO2 and ZnO under sunlight irradiation. Chem. Phys. Lett. 443, 342–346.

Sylvain, F., Grimont, P., 2006. The Genu s Klebsiella. Prokaryotes 6, 159–196.

Tang, Y.-W., Stratton, C.W., 2006. Advanced Techniques in Diagnostic Microbiology, vol. 7. Springer.

Uppal, H. et al, 2017. Study of cyanide removal from contaminated water using zinc peroxide nanomaterial. J. Environ. Sci. (China) 55, 76–85.

Vinotha, V. et al, 2019. Synthesis of ZnO nanoparticles using insulin-rich leaf extract: Anti-diabetic, antibiofilm and anti-oxidant properties. J. Photochem. Photobiol. B Biol. 197, 111541.

Walker, R.D., 1999. Standards for antimicrobial susceptibility testing. Am. J. Vet. Res. 60.

Wang, L., Hu, C., Shao, L., 2017. The-antimicrobial-activity-of-nanoparticles–present-situati. Int. J. Nanomed. 12, 1227–1249.

Wolanov, Y., Prikhodchenko, P.V., Medvedev, A.G., Pedahzur, R., Lev, O., 2013. Moderate pH. Environ. Sci. Technol. 47, 8769–8774.

Zhao, J., Fan, B., Wu, Z., Xu, M., Luo, Y., 2015. Serum zinc is associated with plasma leptin and Cu-Zn SOD in elite male basketball athletes. J. Trace Elem. Med. Biol. 30, 49–53.

Zn, M., 2014. Room temperature conversion of metal oxides (MO, M = Zn, Cd and Mg) to peroxides: insight into a novel, scalable and recyclable synthesis leading to their lowest decomposition temperatures. CrystEngComm 1050–1055. https://doi.org/10.1039/c3ce42276c.